bioRxiv preprint doi: https://doi.org/10.1101/2022.10.02.510516; this version posted October 4, 2022. The copyright holder for this preprint (which was not certified by peer review) is the author/funder, who has granted bioRxiv a license to display the preprint in perpetuity. It is made available under aCC-BY-NC-ND 4.0 International license.

On the origins of phenotypic parallelism in benthic and limnetic stickleback

Laura L. Dean[1]*, Isabel Santos Magalhaes[1,2], Daniele D'Agostino[1,3] Paul Hohenlohe[4] and Andrew D. C. MacColl[1]

[1]School of Life Sciences, The University of Nottingham, University Park, Nottingham, NG7 2RD, UK

[2]School of Health and Life Sciences, Whitelands College, University of Roehampton, London SW15 4JD, UK

[3]Water Research Center, New York University Abu Dhabi, PO Box 129188, Abu Dhabi, United Arab Emirates

[4]Institute for Bioinformatics and Evolutionary Studies, Department of Biological Sciences, University of Idaho, Moscow, ID, USA.

Correspondence: lldean18@gmail.com

bioRxiv preprint doi: https://doi.org/10.1101/2022.10.02.510516; this version posted October 4, 2022. The copyright holder for this preprint (which was not certified by peer review) is the author/funder, who has granted bioRxiv a license to display the preprint in perpetuity. It is made available under aCC-BY-NC-ND 4.0 International license.

Abstract

Rapid evolution of similar phenotypes in similar environments, giving rise to *in situ* parallel adaptation, is an important hallmark of ecological speciation. However, what appears to be *in situ* adaptation can also arise by dispersal of divergent lineages from elsewhere. We test whether two contrasting phenotypes repeatedly evolved in parallel, or have a single origin, in an archetypal example of ecological adaptive radiation: benthic-limnetic three-spined stickleback (*Gasterosteus aculeatus*) across species-pair and solitary lakes in British Columbia. We identify two genomic clusters across freshwater populations, which differ in benthic-limnetic divergent phenotypic traits and separate benthic from limnetic individuals in species pair lakes. Phylogenetic reconstruction and niche evolution modelling both suggest a single evolutionary origin for each of these clusters. We detected strong phylogenetic signal in benthic-limnetic divergent traits, suggesting they are ancestrally retained. Accounting for ancestral state retention, we identify local adaptation of body armour due to the presence of an intraguild predator, the sculpin (*Cottus asper*) and environmental effects of lake depth and pH on body size. Taken together, our results imply a predominant role for retention of ancestral characteristics in driving trait distribution, with further selection imposed on some traits by environmental factors.

bioRxiv preprint doi: https://doi.org/10.1101/2022.10.02.510516; this version posted October 4, 2022. The copyright holder for this preprint (which was not certified by peer review) is the author/funder, who has granted bioRxiv a license to display the preprint in perpetuity. It is made available under aCC-BY-NC-ND 4.0 International license.

Introduction

Parallel occurrence of adaptive phenotypes across similar but geographically separate environments has long fascinated evolutionary biologists. There are two main mechanisms which can explain such a pattern. First, novel adaptive phenotypes may evolve rapidly and repeatedly in response to new ecological opportunity i.e. parallel ecological speciation [1]. Alternatively, an adaptive phenotype may arise in a single location and disperse into and or persist only in suitable environments [2-4]. Although these two mechanisms result in the same pattern, they reflect extremely different evolutionary histories: multiple evolutionary origins of the same phenotype vs a single origin. It is therefore necessary to determine which evolutionary history is responsible for apparent parallelism if we are to understand it. There are many definitions for parallel and convergent evolution [5, 6], but here we focus on whether similar phenotypic adaptations share an ancestral genetic basis.

Parallel ecological speciation may involve multiple *de novo* mutations, each of which may lead to a similar phenotype but by a slightly different mechanism. In this instance it is easy to conclude multiple independent origins. However, evolution is not linear but often reticulated, and, in many cases, parallel ecological adaptation may involve repeated reuse of long-standing genetic variation i.e. the same, potentially ancient mutation can be introduced to multiple independent populations via admixture [7]. In this case, parallel populations may be young, and have multiple origins, but the mutations responsible for adaptation are shared and may be much older. This scenario is extremely difficult to differentiate from a scenario in which parallel populations themselves have a single origin [8], but it is critical that we attempt to do so in order to understand the underlying processes that shape evolution.

The benthic-limnetic axis of stickleback in British Columbia ('BC'), Canada, is an archetypal example of ecological divergence and speciation [9-14]. It separates bottom-dwelling, benthic

bioRxiv preprint doi: https://doi.org/10.1101/2022.10.02.510516; this version posted October 4, 2022. The copyright holder for this preprint (which was not certified by peer review) is the author/funder, who has granted bioRxiv a license to display the preprint in perpetuity. It is made available under aCC-BY-NC-ND 4.0 International license.

53 individuals, which feed predominantly on macroinvertebrates, from pelagic fish, feeding
54 mostly on zooplankton [15-17]. These two freshwater ecotypes are characterised by heritable
55 differences in body size, shape, trophic morphology and body armour, which confer fitness
56 advantages in their corresponding habitats [18-20]. In BC, stickleback occur both as
57 sympatric benthic-limnetic species pairs and solitary populations that possess phenotypes
58 along the benthic-limnetic axis [9, 21-24]. Previous work has identified patterns of
59 parallelism in adaptive genomic divergence across benthic-limnetic species pairs, but closer
60 genetic affinity within lakes at neutral markers [21, 22, 25]. This work has tentatively led to
61 the conclusion that benthic and limnetic phenotypes evolved repeatedly and independently in
62 multiple lakes [21, 25, 26]. However, gene flow occurs to some extent in all benthic-limnetic
63 species pairs [27, 28], and even low levels of gene flow quickly erode genetic differences at
64 neutral loci, making it impossible to separate patterns of recent *in situ* ecological speciation
65 from those derived from secondary contact of much older independent lineages [29]. Little
66 investigation has so far been conducted beyond the species pairs, which coexist in only a
67 handful of lakes [30], but see [31]. Populations in solitary lakes have far less opportunity for
68 gene flow and thus will likely give a more reliable estimate of the evolutionary history of
69 benthic and limnetic ecotypes.

70 We investigate whether benthic-limnetic divergence in BC stickleback likely has a single or
71 multiple evolutionary origins. We first characterise genomic and phenotypic divergence
72 across populations and show that all freshwater individuals fall within one of two genomic
73 clusters, one of which exhibits a more benthic phenotype, and the other, a more limnetic
74 phenotype. We construct a maximum likelihood phylogeny using a stringently filtered
75 dataset, removing all known QTL in stickleback, and test for phylogenetic signal in
76 ecologically relevant phenotypic traits. We construct a microevolutionary adaptive landscape
77 for the BC radiation using recently available niche modelling techniques [32] to identify the

bioRxiv preprint doi: https://doi.org/10.1101/2022.10.02.510516; this version posted October 4, 2022. The copyright holder for this preprint (which was not certified by peer review) is the author/funder, who has granted bioRxiv a license to display the preprint in perpetuity. It is made available under aCC-BY-NC-ND 4.0 International license.

best fitting model of benthic-limnetic trait evolution. Finally, accounting for any phylogenetic signal, we test for relationships between phenotype and environment to detect signals of true ecological adaptation.

Results

We collected stickleback, and environmental parameters from 21 lakes surrounding the Strait of Georgia, BC (Figure 1), including two species pair lakes, two coastal locations (representing putative marine ancestors) and 17 solitary freshwater lakes (Table S1). We collected phenotypic data for key benthic-limnetic divergent traits (methods) for approximately 32 individuals (mean = 31.5, SE = 2.4) and generated RAD-seq genomic data [13], for approximately 16 individuals (mean = 15.9, SE = 0.9), from each lake, 333 individuals in total. This resulted in a master genomic dataset of 12,756 SNPs, which was subject to further filtering for some analyses (Table 1).

bioRxiv preprint doi: https://doi.org/10.1101/2022.10.02.510516; this version posted October 4, 2022. The copyright holder for this preprint (which was not certified by peer review) is the author/funder, who has granted bioRxiv a license to display the preprint in perpetuity. It is made available under aCC-BY-NC-ND 4.0 International license.

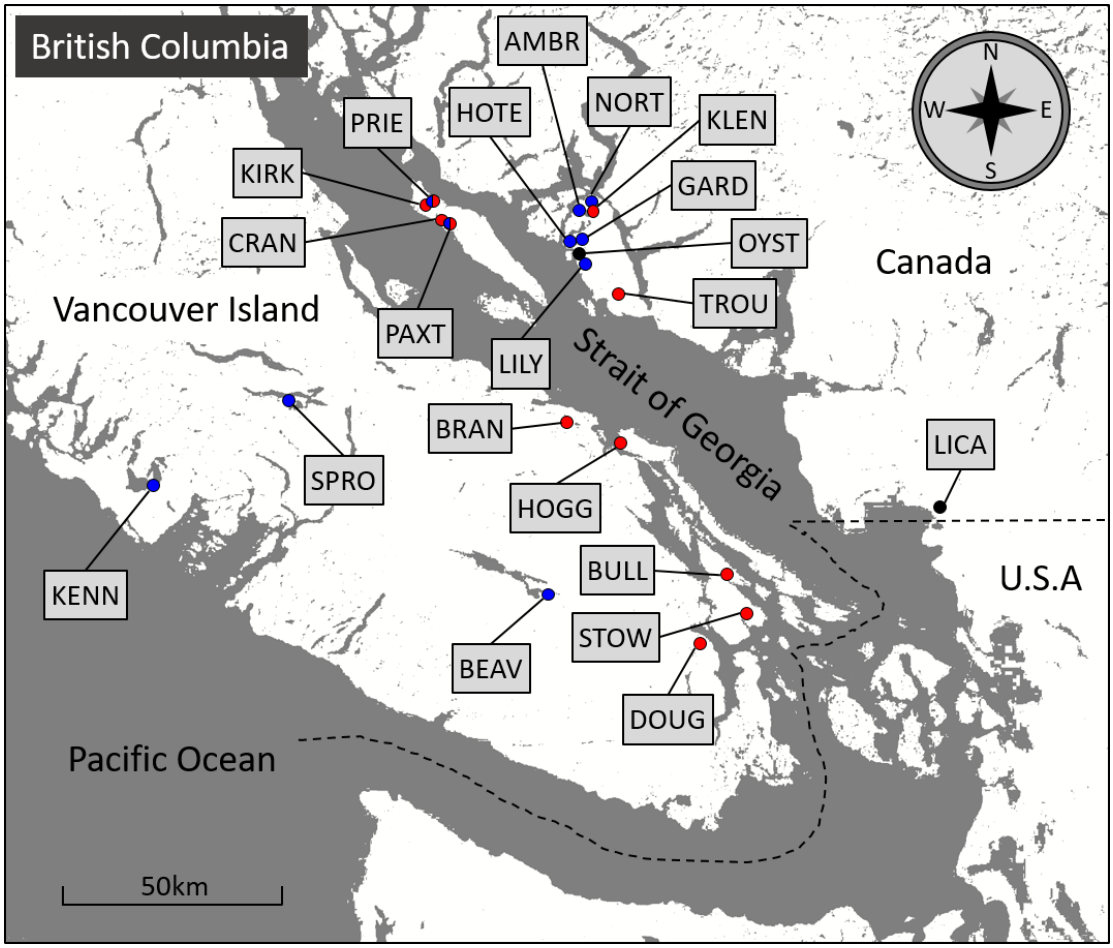

Figure 1. Map of sampling locations in British Columbia. Sample sites are indicated by circles and their associated lake ID. Black circles indicate marine populations, blue circles indicate populations in cluster 1 of our genomic analyses and red circles, cluster 2. Red and blue semi-circles indicate species-pair populations containing individuals from both clusters 1 and 2. The dashed line represents the border between Canada and the USA.

Genomic divergence

We used two methods to quantify clustering within the genomic data. Firstly, a co-ancestry matrix in fineRADstructure [33] (dataset 1, 12,756 SNPs) identified two genomic clusters across all populations (Figure 2A), one incorporating the marine populations and approximately half of the freshwater populations (cluster 1), and the other comprising the rest of the freshwater lakes (cluster 2). Although marine populations formed part of cluster 1, they are considered separately here and in all further analyses because their presence in shallow

bioRxiv preprint doi: https://doi.org/10.1101/2022.10.02.510516; this version posted October 4, 2022. The copyright holder for this preprint (which was not certified by peer review) is the author/funder, who has granted bioRxiv a license to display the preprint in perpetuity. It is made available under aCC-BY-NC-ND 4.0 International license.

coastal areas is transient and they likely represent the ancestral phenotypic state of all freshwater populations [7]. Secondly, we conducted a principal coordinate analysis (PCoA, dataset 2, 9668 SNPs). The same two broad genomic clusters (1 and 2) were identified by PCoA analysis, separating along PCo1 (9% of total variation, Figure 2B).

To further investigate the genomic properties of cluster 1 and 2 differentiation, we conducted a linkage disequilibrium network analysis (LDna) using the LDna R package (dataset 1, 12,756 SNPs). The resulting LD network contained twelve linkage clusters, each of which is likely a signature of a different evolutionary phenomenon [34]. Principal component analysis (PCA) on the SNPs from each cluster revealed a group of 60 SNPs, spread across 17 of the 21 chromosomes in the stickleback genome, associated with cluster 1 – cluster 2 separation. Of these 60 SNPs, 28 fell directly within genes (Table S2). Most other LD clusters only separated single populations from all others, likely reflecting local patterns of selection and drift and none of the LD clusters separated marine and freshwater adapted populations (Figures S1 and S2).

bioRxiv preprint doi: https://doi.org/10.1101/2022.10.02.510516; this version posted October 4, 2022. The copyright holder for this preprint (which was not certified by peer review) is the author/funder, who has granted bioRxiv a license to display the preprint in perpetuity. It is made available under aCC-BY-NC-ND 4.0 International license.

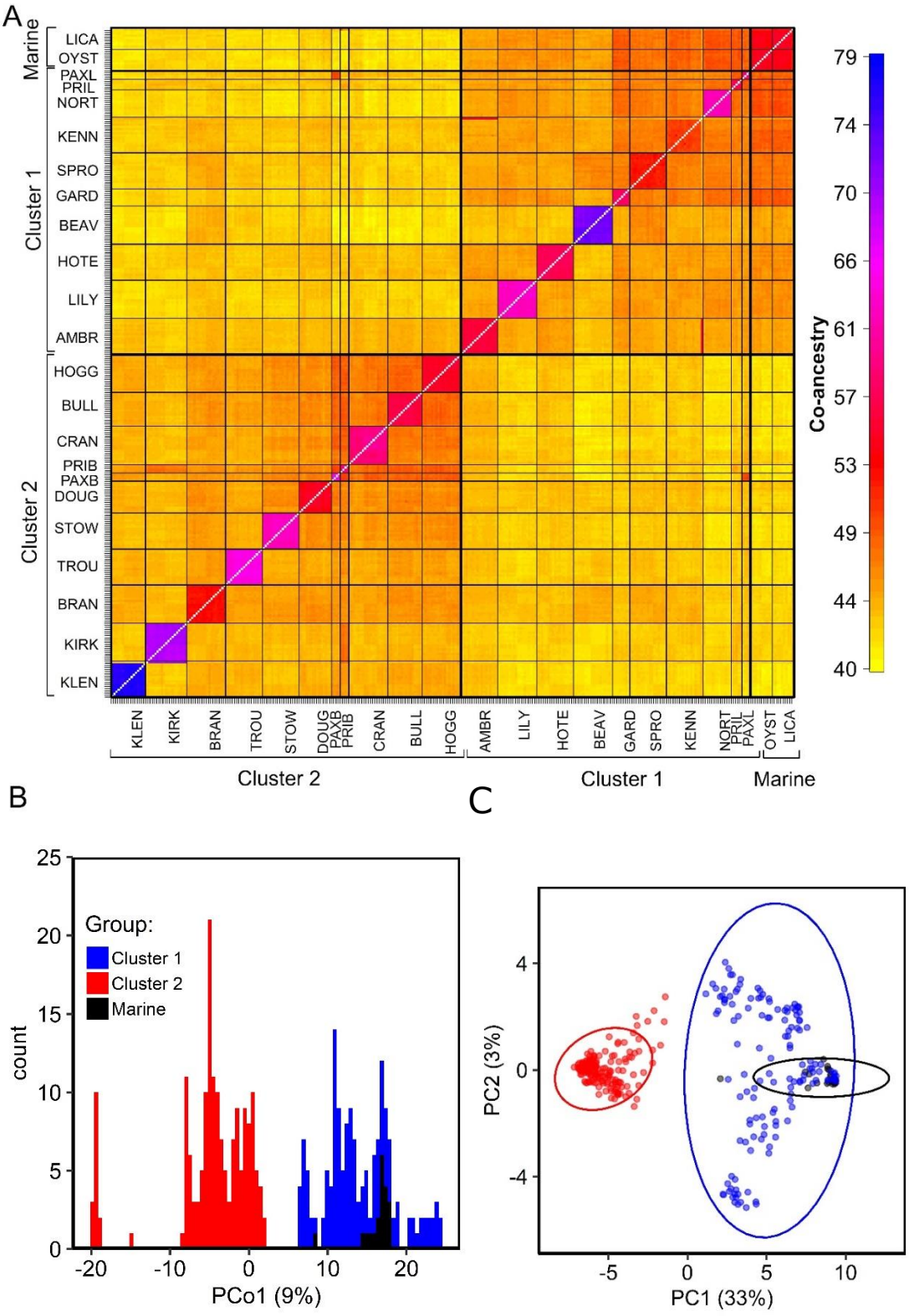

Figure 2. Genetic structure across BC stickleback populations. (A) Co-ancestry matrix of BC stickleback populations, using fineRADstructure. Thin black lines separate populations and thick black lines separate the broader genetic clusters. (B) Distribution of BC stickleback along the first principal coordinate of a genomic PCoA (dataset 2, 9668 SNPs). (C)

bioRxiv preprint doi: https://doi.org/10.1101/2022.10.02.510516; this version posted October 4, 2022. The copyright holder for this preprint (which was not certified by peer review) is the author/funder, who has granted bioRxiv a license to display the preprint in perpetuity. It is made available under aCC-BY-NC-ND 4.0 International license.

Distribution of BC individuals in a PCA of 60 linked SNPs comprising linkage cluster 10, identified by LDna.

Phenotypic divergence

To determine whether the genomic clusters differed phenotypically, we analysed differences in group means for important benthic-limnetic divergent phenotypic traits: weight, gill raker length and number, armour PC1 (increasing size of all armour variables and increasing lateral plate number, explaining 70.4% of body armour variation [methods]) and shape PC1 (describing shape changes associated with benthic and limnetic habitats, such as eye size, body depth and mouth length, explaining 23.2% of body shape variation [35, 36]). There were differences in phenotype between the three groups for all phenotypic traits (Table S3). For most traits, clusters 1 and 2 differed from marine fish, and for all traits except for body weight, clusters 1 and 2 differed from each other (Table S4, Figure 3A-E). Cluster 1 had a typically limnetic phenotype [35, 36] with a smaller size, longer, more numerous gill rakers, more body armour, a larger pelvis relative to spine length, and a more streamlined, slender body shape than cluster 2, which had a much more benthic phenotype (Figure 3A-E).

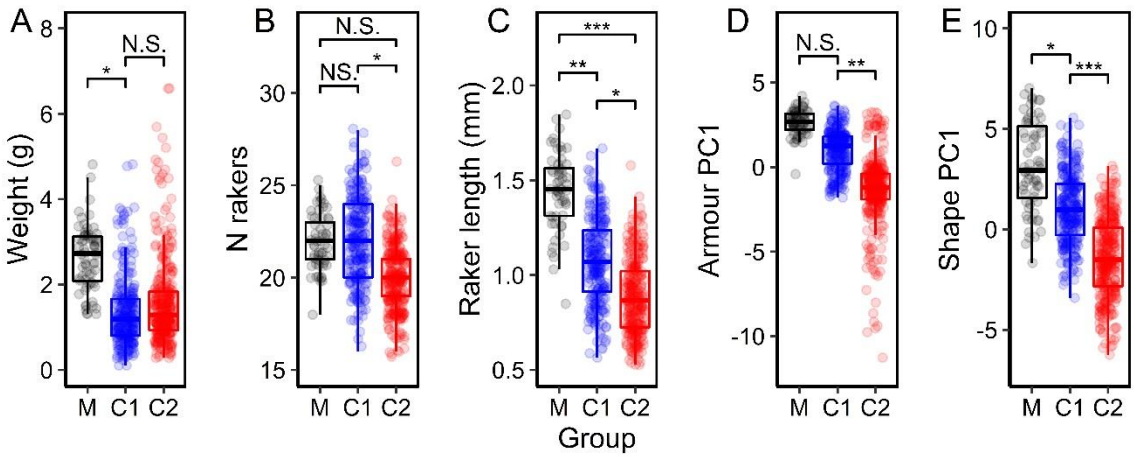

Figure 3. (A) – (E) Phenotypic differences between marine fish and two freshwater genetic clusters. Circles represent individuals. Abbreviations: M – marine, C1 – cluster 1, C2 – cluster 2. Brackets and asterisks indicate significance thresholds of post-hoc estimated marginal means tests between groups: NS. indicating $p > 0.05$, ** indicating $p < 0.01$ and *** indicating $p < 0.001$. All p values were adjusted for multiple comparisons.

bioRxiv preprint doi: https://doi.org/10.1101/2022.10.02.510516; this version posted October 4, 2022. The copyright holder for this preprint (which was not certified by peer review) is the author/funder, who has granted bioRxiv a license to display the preprint in perpetuity. It is made available under aCC-BY-NC-ND 4.0 International license.

Phylogeny

Phylogenetic reconstruction for population-level genomic data can be notoriously problematic as numerous factors, including ongoing and / or historic gene flow can mask true phylogenetic signal in the data [37, 38]. To minimise bias in our analysis, we first filtered our master dataset (dataset 1, 12,756 SNPs) to remove all known QTL in stickleback (leaving 8351 SNPs, see methods), and then filtered for linkage disequilibrium ($R^2 > 0.2$, leaving 6215 SNPs, dataset 3). We constructed a maximum likelihood phylogeny for all populations using RAxML. Consistent with the co-ancestry and PCoA analyses, the topology showed clusters 1 (more limnetic phenotype) and 2 (more benthic phenotype) at opposite ends of the tree, with marine fish most closely related to cluster 1 (Figure 4A). The two species-pair lakes both contained limnetic individuals whose closest relatives were in cluster 1 (PAXL and PRIL), and benthic individuals whose closest relatives were in cluster 2 (PAXB and PRIB, Figure 4A).

We also performed a topology weighting analysis on a subset of populations selected specifically to test the likelihood that the phenotypes associated with clusters 1 and 2 could have evolved repeatedly *in situ*. Topology weighting is a means by which to quantify relationships between taxa that are not necessarily monophyletic. It determines how support for each possible topology varies across the genome and allows quantification of the overall proportion of the genome which supports each possible tree. This allowed us to identify multiple highly supported phylogenies so that we could determine whether any of those with high support involved a model in which the two clusters arose more than once. It also allowed us to quantify what proportion of the genome supports our most likely topology, and how big the difference is between this and the level of support for the next most likely tree. To do this, we selected two populations from each of two locations approximately 100km apart and separated by the Georgia Strait. Each location contained a cluster 1 and 2

bioRxiv preprint doi: https://doi.org/10.1101/2022.10.02.510516; this version posted October 4, 2022. The copyright holder for this preprint (which was not certified by peer review) is the author/funder, who has granted bioRxiv a license to display the preprint in perpetuity. It is made available under aCC-BY-NC-ND 4.0 International license.

168 population occurring reasonably close together which, under a model based purely on
169 geography, would be predicted to be more closely related. One marine individual was used as
170 an outgroup. The topology with the highest weighting across all 50bp sliding windows
171 (topology 8) was concordant with the maximum likelihood phylogeny, with the two cluster 2
172 populations (DOUG and KLEN) forming a monophyletic clade and each cluster 1 population
173 splitting off earlier, deeper to the root (Figure 4C). The topology with the second highest
174 weightings (topology 7) was also concordant, and just involved a switching of the order in
175 which the cluster 1 populations split from the root. The simple geographical hypothesis, with
176 the two pairs of populations nearest to one another being most closely related (topology 3)
177 received very little support. The highest ranking topology had more than twice the
178 proportional support that the second most likely topology had, suggesting that there is a
179 strong genome-wide signal in favour of the maximum likelihood topology.

bioRxiv preprint doi: https://doi.org/10.1101/2022.10.02.510516; this version posted October 4, 2022. The copyright holder for this preprint (which was not certified by peer review) is the author/funder, who has granted bioRxiv a license to display the preprint in perpetuity. It is made available under aCC-BY-NC-ND 4.0 International license.

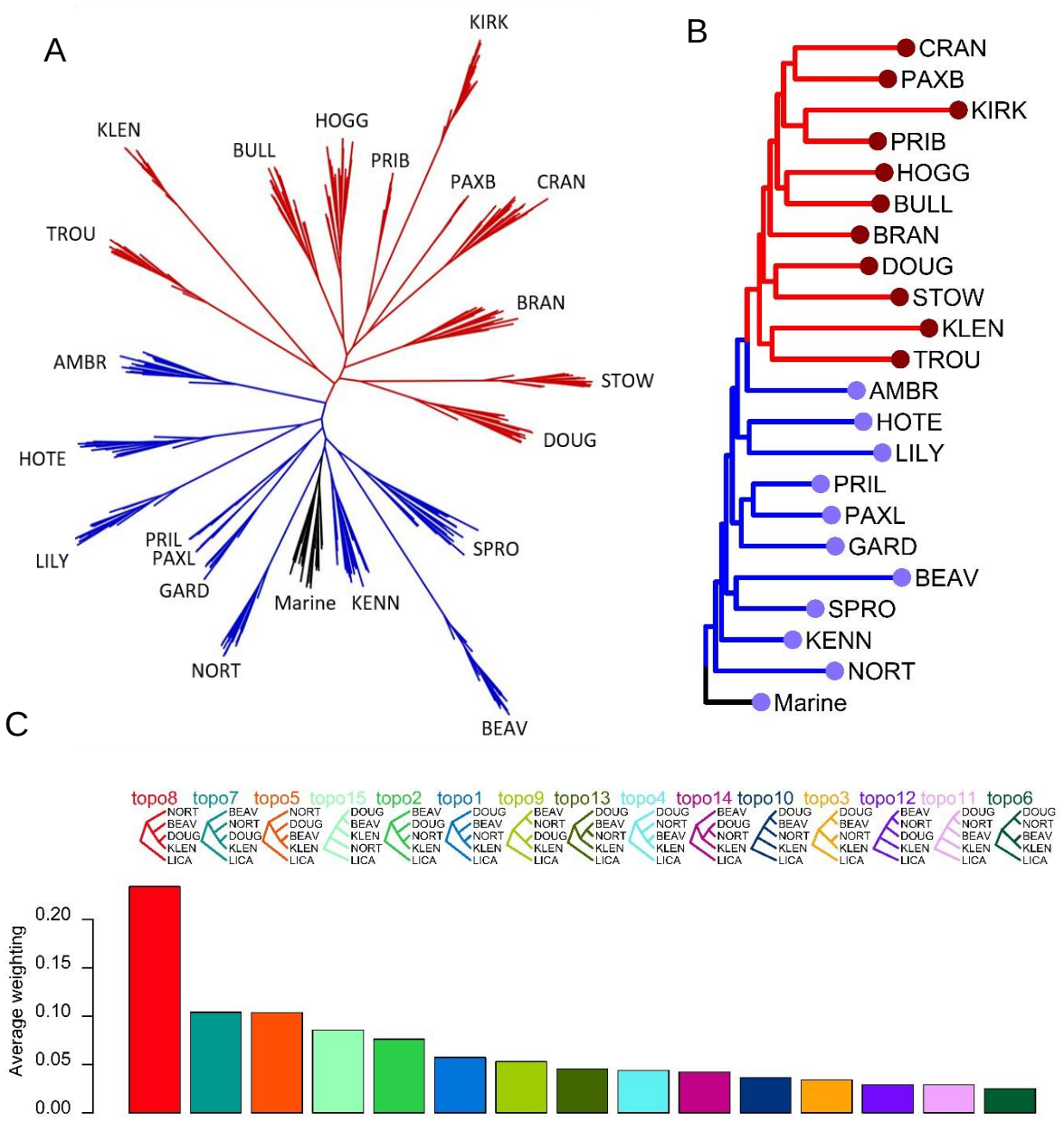

Figure 4. (A) Maximum likelihood phylogeny of 333 BC stickleback. Black indicates marine; blue, cluster 1 and red, cluster 2. (B) The same phylogeny as (A) with monophyletic populations collapsed into single tips. Branch colours in (B) denote the same as in (A). Coloured circles at branch tips represent two independent selection regimes, detected in the optimal model of niche evolution (R package: SURFACE). In both phylogenies species pairs are divided into benthic (PAXB, PRIB) and limnetic (PAXL, PRIL) populations. (C) Mean weightings for all possible topologies for four freshwater populations: two from cluster 1, NORT and BEAV; and two from cluster 2, DOUG and KLEN, with a single individual from the marine population LICA as the outgroup.

bioRxiv preprint doi: https://doi.org/10.1101/2022.10.02.510516; this version posted October 4, 2022. The copyright holder for this preprint (which was not certified by peer review) is the author/funder, who has granted bioRxiv a license to display the preprint in perpetuity. It is made available under aCC-BY-NC-ND 4.0 International license.

Phylogenetic signal

If benthic and limnetic phenotypes had resulted from repeated, rapid adaptive divergence, phylogenetic signal (the tendency for more closely related individuals to share phenotypes) would be obscured, and trait distributions would instead mimic the adaptive landscape — i.e. variation in the relevant environmental characteristics. Therefore, we tested a null model that traits would be distributed randomly with respect to phylogeny, and an association of trait distribution with population-level relatedness was taken as evidence that benthic and limnetic niches were conserved from the ancestral state [39-41].

We estimated phylogenetic signal at the population level, using mean phenotypic trait data, and collapsing nodes in the phylogeny by population (with the two marine populations grouped into a single node, as they lacked monophyly), using the R package: PhyloSignal. We also tested five simulated traits that had no true association with phylogeny. We identified phylogenetic signal in all five real phenotypic traits: weight, gill raker number, gill raker length, armour PC1 and shape PC1 (p-values < 0.05, Table 2). None of the five randomly simulated traits showed phylogenetic signal (p-values > 0.05, Table 2).

Niche evolution modelling

Niche evolution modelling combines phylogenetic information with the distribution of phenotypic traits across the tree to identify the most likely number and location of selection regimes imposed across the whole phylogeny. It also identifies the number of instances of convergence (where the same regime appears multiple times across the tree). If the benthic phenotype had evolved repeatedly and independently across the phylogeny, niche evolution modelling should identify multiple instances of convergence of a benthic selection regime. We performed niche evolution modelling using the R package SURFACE [32]. We ran SURFACE using the same collapsed phylogeny and associated trait data that were used to

bioRxiv preprint doi: https://doi.org/10.1101/2022.10.02.510516; this version posted October 4, 2022. The copyright holder for this preprint (which was not certified by peer review) is the author/funder, who has granted bioRxiv a license to display the preprint in perpetuity. It is made available under aCC-BY-NC-ND 4.0 International license.

estimate phylogenetic signal. The best fitting model involved two different selection regimes across the phylogeny (Figure 4B). The first included all marine and cluster 1 populations, and the second, all cluster 2 populations. The best fitting model included no instances of convergence between selection regimes, i.e. each independent regime appeared only once across the phylogeny.

Relationship between phenotype and environment

To test for phenotype – environment relationships, we used linear mixed models, following a phylogenetic generalised least squares (PGLS) approach so that phylogenetic signal could be accounted for and fitted to the population means of phenotypic traits in R. Marine fish were excluded from all phenotype – environment modelling, because of the difficulty of measuring the environment of migratory marine fish. We found that freshwater fish had more body armour in the presence of sculpin (adjusted p-value < 0.05, Table S5), and fish were heavier in deeper lakes and lakes with a higher pH (adjusted p-values < 0.01 and < 0.05, respectively). Lake surface area and calcium concentration did not affect any aspect of phenotype and none of the environmental variables we measured affected the number of gill rakers, the length of gill rakers or shape PC1 (Table S5).

bioRxiv preprint doi: https://doi.org/10.1101/2022.10.02.510516; this version posted October 4, 2022. The copyright holder for this preprint (which was not certified by peer review) is the author/funder, who has granted bioRxiv a license to display the preprint in perpetuity. It is made available under aCC-BY-NC-ND 4.0 International license.

Discussion

The repeated occurrence of similar phenotypes in geographically isolated but similar environments has several possible evolutionary explanations. Perhaps this pattern results from parallel ecological speciation, or maybe similar phenotypes have a single origin and have subsequently become widely dispersed into suitable habitats. It is impossible to separate these different models using only phenotypic data or small numbers of genetic markers, and remains difficult even with genomic data. Nevertheless, it is important that we attempt to do so, because of the consequences for our understanding of evolution. Parallel evolution has been implicated in the global adaptation of stickleback to freshwater [21], but recent analyses suggest that this is unlikely outside of the Eastern Pacific [42]. Furthermore, there are a number of other cases in which conclusions of parallel ecological speciation have been called into question by the confounding possibility of a single evolutionary origin followed by migration and gene flow [29].

We investigated the evolutionary origins of divergent phenotypes in a classic model system for adaptive radiation and ecological speciation. We find strong evidence for a monophyletic clade of stickleback with a benthic phenotype distributed across freshwater lakes in the southern Georgia Strait region of BC. The evidence strongly suggests that this clade has a single evolutionary origin, and is derived from a local ancestor with a limnetic phenotype. The benthic clade also encompasses benthic fish from two benthic-limnetic species pairs. Our results are consistent with a single origin for benthic fish in BC rather than repeated independent evolution of the benthic phenotype in multiple lakes. This contradicts the currently favoured model for the evolution of benthic and limnetic stickleback in BC [21, 22, 25], highlighting the challenging nature of phylogenetic reconstruction at the population level.

bioRxiv preprint doi: https://doi.org/10.1101/2022.10.02.510516; this version posted October 4, 2022. The copyright holder for this preprint (which was not certified by peer review) is the author/funder, who has granted bioRxiv a license to display the preprint in perpetuity. It is made available under aCC-BY-NC-ND 4.0 International license.

Many factors, such as incomplete lineage sorting, hybridization, gene duplication, natural selection and recombination can lead to genealogical discordance in estimations of phylogenetic relationships [43]. Resolving the true relationships between divergent groups can therefore be challenging and require a large number of genetic markers. Much of the current research on benthic and limnetic stickleback in BC has been based only on mitochondrial haplotypes [25] or relatively small SNP sets [21], and has largely been restricted to species pairs. In species pairs, multiple QTL regions are repeatedly responsible for benthic adaptation [21, 44, 45], which is consistent with a single benthic origin, but neutral SNPs imply closer genetic affinity of benthics and limnetics within lakes [21], consistent with multiple independent origins. However, elevated levels of genetic similarity at neutral markers in species pairs would be expected even with low levels of gene flow and thus may not reflect true phylogenetic relationships [27]. Clearly, it is important also to consider relationships in solitary populations, where opportunity for gene flow is greatly reduced. Harer et al. [31] looked at both species pairs and solitary populations and identified considerable genomic parallelism in the former but not the latter. However, they define the benthic-limnetic spectrum in solitary populations solely using lake surface area, which correlates only weakly with phenotype, and does not account for differences in lake depth and the presence of specific predators, which also have a major influence on the availability of benthic and limnetic niches to stickleback [46].

We identify a monophyletic lineage within BC stickleback, which has a consistently benthic phenotype when compared with other freshwater or marine populations in BC. Some argument remains among evolutionary biologists about whether pervasive, genome-wide selection, can overwhelm the signal from other markers and obscure tree topologies [43, 47]. Sculpin (*Cottus asper*) are an intraguild predator of stickleback, which, when present, select for a more limnetic phenotype [48, 49]. Our results were consistent with this as we identified

bioRxiv preprint doi: https://doi.org/10.1101/2022.10.02.510516; this version posted October 4, 2022. The copyright holder for this preprint (which was not certified by peer review) is the author/funder, who has granted bioRxiv a license to display the preprint in perpetuity. It is made available under aCC-BY-NC-ND 4.0 International license.

an effect of sculpin presence on body armour after accounting for phylogenetic signal in our analysis. However, we find the possibility that selection from sculpin obscures the true relationships between populations in our phylogeny unlikely for a number of reasons. Firstly, such a phenomenon is certainly possible in studies using only a small number of markers [50], but with many thousands of unlinked genetic markers, such as in this case, the probability of selection overwhelming the signal from neutral markers is very low [47, 51]. Secondly, recent modelling suggests that even with strong selection affecting 10-20% of markers, in most instances, phylogenetic inference remains robust to the effects of selection [52]. Selection from sculpin likely affects less than 2% of the genome [48] and thus is at least an order of magnitude smaller in effect size than would be necessary to obscure the true tree topology in this case. Furthermore, sculpin were present in some lakes containing the benthic clade and not in all lakes containing the limnetic clade. Thus, the genomic groups identified here do not simply mirror the occurrence of this selective agent, but rather represent a deeper set of ancestral relationships.

If the benthic phenotype in BC has a single origin, a clear question that requires explanation is how this ecotype spread across BC? Although the lakes containing stickleback in BC are not particularly widespread, they are physically separated by land or ocean, which likely makes dispersal a challenge for freshwater stickleback. We speculate that evidence for a large flood (~500km^3 of water) in the Fraser River valley, dated approximately to the end of the Pleistocene and caused by the failure of a large ice dam [53], could provide an explanation. The estimated extent of the flood across the southern Georgia Strait is very similar to the current known distribution of benthic stickleback in BC, raising the tantalising possibility that it may have been responsible for the spread of the benthic lineage of stickleback from a palaeolake in the Fraser Valley, consistent with previous inference about the evolution of Eastern Pacific freshwater stickleback [42].

bioRxiv preprint doi: https://doi.org/10.1101/2022.10.02.510516; this version posted October 4, 2022. The copyright holder for this preprint (which was not certified by peer review) is the author/funder, who has granted bioRxiv a license to display the preprint in perpetuity. It is made available under aCC-BY-NC-ND 4.0 International license.

Our investigations have shown that the well-studied benthic-limnetic species pairs should be understood as part of a broader radiation along the benthic-limnetic axis in BC. We highlight the need to consider carefully all possible explanations for the occurrence of parallel phenotypes if we are to achieve a proper understanding of the evolutionary processes that mediate divergence. Stickleback are clearly capable of remarkably rapid ecological adaptation [54-58], but we have shown that the retention of ancestral characteristics can also be important in explaining the distribution of divergent phenotypes. This has significant implications for how we think about the process of evolution and raises the possibility that other model examples of *in situ* ecological adaptation may also result from dispersal rather than convergence.

Declaration of Interests

The authors declare no competing interests.

Acknowledgements

The authors would like to thank the Schluter lab for assistance with fieldwork and collection permits and Dolph Schluter for useful comment on previous drafts of the manuscript, Steve Vamosi for access to lake habitat data, Ann Lowe for assisting with the DNA extractions, and Muayad Mahmud and Becca Young for assistance with phenotyping. We would also like to thank Mark Ravinet for providing useful suggestions to improve the analyses and towards drafting the manuscript. Analyses of genomic data were conducted using the University of Nottingham's on premise, high performance computer service, Augusta.

This work was funded by NERC grants NE/J02239X/1 and NE/R00935X/1.

bioRxiv preprint doi: https://doi.org/10.1101/2022.10.02.510516; this version posted October 4, 2022. The copyright holder for this preprint (which was not certified by peer review) is the author/funder, who has granted bioRxiv a license to display the preprint in perpetuity. It is made available under aCC-BY-NC-ND 4.0 International license.

Tables

Table 1

SNP datasets. Details of the SNP datasets used in genomic analyses.

Dataset	N lakes	N individuals	N SNPs	LD thinned	Known QTL removed
dataset 1	21	333	12,756	✗	✗
dataset 2	21	333	9668	✓	✗
dataset 3	21	333	6215	✓	✓
dataset 4	5	53	9668	✓	✗

N: number, LD thinned: SNPs with $r^2 > 0.2$ removed, Known QTL: SNPs identified as falling within known QTL regions [59].

Table 2

Phylogenetic signal in real and simulated phenotypic traits. Table shows estimates of phylogenetic signal (Pagel's λ) and their associated *p*-values. *P*-values < 0.05 are highlighted in bold.

Trait	Pagel's λ	*p*-value
Weight	1.5881	**0.0421**
Number of gill rakers	2.1535	**0.0010**
Mean gill raker length	1.6492	**0.0032**
Armour PC1	0.9667	**0.0269**
Shape PC1	1.3647	**0.0010**
Random 1	0.0001	1.0000
Random 2	0.0001	1.0000
Random 3	0.0001	1.0000
Random 4	0.0001	1.0000
Random 5	0.0001	1.0000

bioRxiv preprint doi: https://doi.org/10.1101/2022.10.02.510516; this version posted October 4, 2022. The copyright holder for this preprint (which was not certified by peer review) is the author/funder, who has granted bioRxiv a license to display the preprint in perpetuity. It is made available under aCC-BY-NC-ND 4.0 International license.

Methods

Samples sites and environmental measurements

A total of 21 lakes surrounding the Strait of Georgia, BC, which were likely to vary substantially in the ecological niches they presented to stickleback (because of variation in environmental factors), were selected for sampling (see Table S1 for detailed sample site information and Figure 1 for a map of sampling locations). This included two lakes, Paxton (PAXT) and Priest (PRIE), known to contain benthic-limnetic stickleback species pairs [16, 26], and two coastal locations accessible from the sea, Oyster lagoon (OYST) and Little Campbell River (LICA), where marine fish are present during the spring breeding season.

The size and depth of a lake largely determine whether both benthic and limnetic habitats are present (in larger deeper lakes) or just benthic (in small, shallow lakes). Therefore, we measured the surface area (km^2) using GoogleEarth and collected data on the mean depth (m) of each lake from either HabitatWizard [60] or from data collected in Vamosi [61], with permission. The presence of other fish species can also determine whether both, one or none of those niches are available to stickleback [61]. Many other fish species occur in BC, some of which are predators and/or competitors of stickleback. Cutthroat trout (*Oncorhynchus clarkii*) and rainbow trout (*Oncorhynchus mykiss*) are major intraguild predators of stickleback, but both occur in both the littoral and pelagic zones [62, 63] and do not eliminate either niche for stickleback and so are not considered further here. Prickly sculpin (*Cottus asper*) are a benthic intraguild predator, and their presence selects for a more limnetic stickleback ecotype [46]. We therefore collected data on the presence/absence of prickly sculpin in all sampling locations from Hutchinson et al. [64], Miller et al. [48], Atkinson [65], Dennenmoser et al. [66] and Vamosi [61] (see Supplementary Material for data sources for each lake).

bioRxiv preprint doi: https://doi.org/10.1101/2022.10.02.510516; this version posted October 4, 2022. The copyright holder for this preprint (which was not certified by peer review) is the author/funder, who has granted bioRxiv a license to display the preprint in perpetuity. It is made available under aCC-BY-NC-ND 4.0 International license.

The pH [67] and dissolved calcium concentrations [68] of lake water have previously been associated with external bony armour in stickleback (a trait which varies between benthic and limnetic ecotypes). Therefore we also measured these variables, the former with a calibrated pH meter (Multi 340i, WTW, Weilheim, Germany) and the latter were obtained by collecting two filtered water samples (one acidified with 2% nitric acid, one frozen) from each lake. The dissolved calcium concentration (to the nearest mg/L) was then measured from the water samples at the Division of Agriculture & Environmental Science at the University of Nottingham by inductively coupled plasma mass spectrometry (ICP-MS).

Stickleback sampling

Stickleback were caught using unbaited minnow traps set overnight from the lake shores during spring of 2015 (all stickleback ecotypes move to the shallows during the spring to breed). Samples of between 10 and 63 individuals (See Table S1 for lake specific sample sizes) were taken from each lake and transported to a rental property in aerated lake water for processing. Immediately prior to processing, fish were euthanised with an overdose of tricaine methanesulfonate ('MS222') (400 mg L^{-1}), and killed by destruction of the brain, in accordance with Schedule One of UK Home Office regulations and with the approval of the University of British Columbia Animal Care Committee (UBC animal care certificate A11-0402). Fin clips were immediately taken and stored in 90% Ethanol for later genomic analyses.

Identification of benthic-limnetic divergence

Phenotypic quantification

Fish sampled from lakes containing species pairs (PAXT and PRIE) were visually classified as benthic or limnetic at the time of capture as well as being later measured for all phenotypic traits.

bioRxiv preprint doi: https://doi.org/10.1101/2022.10.02.510516; this version posted October 4, 2022. The copyright holder for this preprint (which was not certified by peer review) is the author/funder, who has granted bioRxiv a license to display the preprint in perpetuity. It is made available under aCC-BY-NC-ND 4.0 International license.

To determine body size, fish were blotted and weighed to the nearest milligram. To assess body shape differences, each stickleback's left side was photographed using a tripod mounted digital SLR camera fitted with a macro lens and macro digital ring flash. Images were scaled, and 13 landmarks were placed on each image using tpsDig, version 2.16 [69]. Landmark data were then exported to MorphoJ, version 1.06d [70]. A Procrustes fit was performed to align specimens by their main axes and remove size and rotation bias. Differences between lakes were identified using a Procrustes ANOVA with lake as the classifier. Allometric variation in body shape was removed by taking the residuals of a multivariate partial least squares regression against log centroid size, and the regression was pooled within lakes because the Procrustes ANOVA indicated differences between group centroids [71]. Regression residuals were exported into R, version 3.5.2 [72], where they were standardised and scaled, and variation in body shape was reduced to a single axis using a principal components analysis (PCA), implemented by singular value decomposition. This principal axis (shape PC1) was used to describe differences in body shape in all further analyses.

To assess differences in body armour, fish were first bleached and then stained with alizarin red to highlight external skeletal structures following standard procedure [73]. Fish were then re-photographed as above, images were scaled, and counts of lateral plate number, alongside measurements of standard length, first and second dorsal spine length, longest plate length, pelvis height, pelvis length and pelvic spine length, were taken (continuous elements to the nearest 0.01mm) using ImageJ, version 1.52a [74]. All continuous armour variables (thus excluding plate number, which was independent of body size in our data set) were size-standardized by taking the residuals of a regression against standard length. Body armour variables were highly correlated, thus we used a principal components analysis (PCA) to reduce variation in body armour variables to a single axis: armour PC1. Armour PC1 was used to describe differences in body armour in all further analyses.

bioRxiv preprint doi: https://doi.org/10.1101/2022.10.02.510516; this version posted October 4, 2022. The copyright holder for this preprint (which was not certified by peer review) is the author/funder, who has granted bioRxiv a license to display the preprint in perpetuity. It is made available under aCC-BY-NC-ND 4.0 International license.

Finally, the left primary gill arch was extracted from each individual. For each gill arch, the total number of gill rakers were counted, and the mean gill raker length was calculated by taking the mean of the length of the first three rakers on each arch, measured to the nearest micrometre.

Genomic SNP analyses

DNA was isolated from fin tissue using Quiagen Blood and Tissue DNA purification kits. RAD-seq data was generated following Magalhaes et al. [75]. BAM files were produced following Magalhaes et al. [75]. Variants were called from per-individual BAM files to create a single VCF file using the Stacks pipeline [76] in Stacks, version 1.47. The POPULATIONS program in Stacks was run with the following filters: SNPs with a minimum depth of coverage < 3 were removed; SNPs present in < 50% of individuals within a population were removed; SNPs with a minor allele frequency < 0.05 were removed; and SNPs that were not present in all of the populations were removed. VCFtools, version 0.1.16 [77], was then used to remove sites with mean depth values (over all individuals) < 6 and > 200, sites with > 25% missing data, sites with a minor allele count over all individuals < 2 and the sex chromosomes. This pipeline produced an overall dataset of 12,756 SNPs for 333 individuals across the 21 lakes (dataset 1). This dataset was then subject to further filtering for some analyses, and detailed information about individual RAD datasets is given in Table 1.

Linkage disequilibrium

Sets of loci that have a tendancy to be inherited together, and thus are highly correlated, tend to be affected by the same evolutionary processes and so contain useful information for identifying the characteristics of the processes affecting each set of linked loci e.g. whether divergence is likely linked to small genomic regions e.g. inversions, or is genome wide. To investigate whether any groups of linked loci would distinguish the genomic clusters

bioRxiv preprint doi: https://doi.org/10.1101/2022.10.02.510516; this version posted October 4, 2022. The copyright holder for this preprint (which was not certified by peer review) is the author/funder, who has granted bioRxiv a license to display the preprint in perpetuity. It is made available under aCC-BY-NC-ND 4.0 International license.

identified in other genomic analyses we performed a linkage disequilibrium network analysis (LDna) using the LDna package in R. The r^2 linkage disequilibrium matrix was generated using dataset 1 (12,756 SNPs) in Plink version 1.9 [78]. For the extractClusters step of LDna the minimum number of edges was set to 100 and Φ was set to five. SNPs in each LD cluster were extracted from dataset 1 using VCFtools, VCF files were read into R using the vcfR package and principal components anaylsis (PCA) of the SNPs in each LD cluster was performed using the adegenet [79] package.

Many genomic tools, however, rely on the assumption that variants are independent and therefore SNPs in linakge diequilibrium must be removed for such analyses. To that end, we estimated linkage disequilibrium across the genome as a whole by calculating pairwise R^2 values in 100kb sliding windows using Plink version 1.9. R^2 values range between 0 (no linkage) and 1 (complete linkage), and therefore a relatively conservative LD threshold was set at $R^2 > 0.2$. Thinning dataset 1 (12,756 SNPs) to unlinked loci resulted in a dataset with 9,668 retained SNPs (dataset 2, Table 1).

Genomic patterns

We used fineRADstructure [33] to construct a co-ancestry matrix using the primary SNP set including all 333 individuals (dataset 1, 12,756 SNPs). Prior filtering for linkage disequilibrium is not necessary for analyses using the RADpainter tool at it efficiently estimates the effective number of loci in mapped data files during the analysis [33]. The fineSTRUCTURE [80] clustering algorithm was run with a burn-in of 100,000 iterations followed by 100,000 sampled iterations and the tree building algorithm was run with a burn-in of 10,000 iterations. We then performed a principal coordinate analysis (PCoA) on the linkage filtered dataset (dataset 2, 9668 SNPs). The PCoA was performed using Elucidean

bioRxiv preprint doi: https://doi.org/10.1101/2022.10.02.510516; this version posted October 4, 2022. The copyright holder for this preprint (which was not certified by peer review) is the author/funder, who has granted bioRxiv a license to display the preprint in perpetuity. It is made available under aCC-BY-NC-ND 4.0 International license.

456 distances with the package adegenet in R. VCF files were converted to genpop format for
457 input to adegenet using PGDSpider, version 2.1.1.5 [81].

458 *Phenotypic divergence*

459 Genomic analyses grouped all fish into two broad genomic clusters, cluster 1 and cluster 2.
460 Although marine fish were grouped with the freshwater fish in cluster 1, they were treated as
461 a third, separate, group in all further analyses. Additionally, they were excluded from most
462 subsequent genetic analyses because their presence in freshwater/coastal areas is transient
463 (they migrate to shallow coastal areas only in the spring to breed) and they represent the
464 likely ancestral state of all freshwater populations [82]. To determine the phenotype of these
465 three groups (marine, cluster 1 and cluster 2), we calculated the mean of each phenotypic
466 variable (weight, number of gill rakers, mean raker length, armour PC1 and shape PC1) for
467 each group. To test whether the means of each phenotypic variable in each of the three
468 groups were significantly different from one another, linear mixed models were performed
469 using the nlme package [83], with lake included as a random effect and group (marine,
470 cluster 1, cluster 2) as a fixed effect. For models showing a significant effect of group, post-
471 hoc pairwise comparisons were performed using estimated marginal means, implemented
472 using the emmeans package [84] in R. P-values for post-hoc comparisons were adjusted for
473 multiple testing using the False Discovery Rate (FDR) method [85].

474 *Phylogenetic analyses*

475 Prior to phylogenetic analysis, we filtered our master dataset (dataset 1) to remove all known
476 QTL in stickleback. Data for QTL were downloaded from Peichel and Marques [59],
477 converted to BED format, and removed from the VCF file using VCFtools. This reduced the
478 number of SNPs from 12,756 to 8351. We then ensured approximate linkage equilibrium of

bioRxiv preprint doi: https://doi.org/10.1101/2022.10.02.510516; this version posted October 4, 2022. The copyright holder for this preprint (which was not certified by peer review) is the author/funder, who has granted bioRxiv a license to display the preprint in perpetuity. It is made available under aCC-BY-NC-ND 4.0 International license.

remaining markers by removing all SNPs with an R^2 value >0.2 using Plink version 1.9. This left 6215 SNPs, dataset 3.

To construct a phylogeny of all sequenced individuals, we used a bootstrapped maximum-likelihood based approach, implemented in RAxML, version 8.2.12 [86]. The VCF file was converted to phylip format for input to RAxML using python version 3.8.2. RAxML was run with a GTR-GAMMA model of substitution rate heterogeneity, automatic bootstrap replicate halting using the autoMRE function and with the default settings for all other parameters.

To assess the robustness of the maximum likelihood phylogeny, we also performed topology weighting using TWISST [87]. Topology weighting was carried out on four freshwater populations, with a single marine sequence (from LICA) as the outgroup. The freshwater populations were selected to contain two pairs of geographically proximal populations, with one pair from either side of the Georgia strait (NORT and BEAV, and DOUG and KLEN), and with one population from each pair falling in cluster 1, the other in cluster 2. Dataset 2 (9668 SNPs) was filtered to contain all individuals from each of the four freshwater populations and a single individual from LICA (TWISST only accepts a single sequence as an outgroup), using VCFtools (dataset 4, 9668 SNPs). The VCF file was converted to .geno format and maximum likelihood trees were estimated in phyml [88] in sliding windows of 50bp using Python 2.7.15 and the scripts available with TWISST. Topology weightings were then computed using Python 3.8.2 and topologies were visualised in R.

Phylogenetic signal in phenotypic traits

To estimate phylogenetic signal, the phylogeny constructed in RAxML was imported into R using the ape package [89], individual nodes were collapsed to leave a single node per population, with the exception of the two marine populations, which were both collapsed into one node using the phytools [90] and phangorn [91] R packages. Phenotypic trait data

bioRxiv preprint doi: https://doi.org/10.1101/2022.10.02.510516; this version posted October 4, 2022. The copyright holder for this preprint (which was not certified by peer review) is the author/funder, who has granted bioRxiv a license to display the preprint in perpetuity. It is made available under aCC-BY-NC-ND 4.0 International license.

(weight, number of gill rakers, mean raker length, armour PC1 and shape PC1) were added to the tree tips, and phylogenetic signal and associated *p*-values for each trait were estimated using the package phylosignal [92]. We used Pagel's λ [93] to estimate phylogenetic signal as this statistic performs well compared to others available and has a low type 1 error rate [39, 94, 95]. *P*-values are calculated using likelihood ratio tests that compare the observed λ statistic with a phylogenetically independent trait distribution. We also simulated data for five additional traits to be distributed randomly with regard to phylogeny. Simulated traits were tested alongside the real phenotypic variables for comparison.

As we aim to detect whether benthic and limnetic characteristics have evolved a single time or repeatedly across the radiation, we also used the R package SURFACE [32] to estimate the most likely number of different selection regimes (*k*) and instances of convergent evolution (*c*) by identify the best fitting model of trait evolution for our phylogeny and associated phenotypic traits. SURFACE begins by fitting a single peak Ornstein-Uhlenbeck (OU) model (which allows for a single adaptive optimum and variation in the parameter α, which describes the strength of selection towards that optimum) by maximum likelihood. It then sequentially adds adaptive peaks to the model in a step-wise process and accepts each more complex model until AIC values are no longer improved. SURFACE then attempts to collapse regimes with the same optima in a process of step-wise backwards selection whereby if multiple optima are the same, the AIC of the model is improved by reducing the number of model parameters. We ran SURFACE using the same collapsed phylogeny and associated trait data that was generated to estimate phylogenetic signal. The tree was converted to ouchtree format and the best fitting model of trait evolution was estimated under an AIC threshold of 0 (any improvement in AIC should be accepted) using the SURFACE R package.

Relationship between phenotype and environment

bioRxiv preprint doi: https://doi.org/10.1101/2022.10.02.510516; this version posted October 4, 2022. The copyright holder for this preprint (which was not certified by peer review) is the author/funder, who has granted bioRxiv a license to display the preprint in perpetuity. It is made available under aCC-BY-NC-ND 4.0 International license.

To investigate associations between environmental characteristics and divergence in phenotypic traits, we used a phylogenetic generalised least squares (PGLS) approach so that phylogenetic signal could be accounted for in the models, using the ape [89], nlme [96] and geiger [97] packages in R. Marine fish were excluded from all phenotype – environment modelling because our main aim was to detect effects in relation to the freshwater benthic and limnetic phenotypes in BC and, although marine fish have a limnetic phenotype, we found them to differ phenotypically from the freshwater limnetic fish in BC. Separate models were run for each phenotypic trait (weight, number of gill rakers, mean gill raker length, armour PC1 and shape PC1). Models were fitted by maximum likelihood and we began with all environmental variables in each model (mean lake depth [m], lake area [km^2], presence/absence of prickly sculpin, pH and calcium concentration [mg/L]). Terms were then removed sequentially, with the least significant terms removed first, until the reduced model was no longer a significant improvement on the fuller model under the $p<0.05$ threshold. Model comparison was conducted using Wald tests. Phylogenetic effects for each phenotypic trait were accounted for in each model following the principles set out in Mazel et al. [98]. We first transformed the phylogeny for each phenotypic trait under a lambda model with lambda specified as the lambda estimate for that phenotypic trait in the phylogenetic signal analyses. The phylogenetic variance-co-variance matrices were computed from the transformed trees using the ape package and converted to correlation matrices, which were used to specify phylogenetic correlation of errors in the models.

bioRxiv preprint doi: https://doi.org/10.1101/2022.10.02.510516; this version posted October 4, 2022. The copyright holder for this preprint (which was not certified by peer review) is the author/funder, who has granted bioRxiv a license to display the preprint in perpetuity. It is made available under aCC-BY-NC-ND 4.0 International license.

548 **References**

549 1. Nosil, P. (2012). Ecological speciation, (Oxford: Oxford University Press).
550 2. Hiller, A.E., Koo, M.S., Goodman, K.R., Shaw, K.L., O'Grady, P.M., and Gillespie,
551 R.G. (2019). Niche conservatism predominates in adaptive radiation: comparing
552 the diversification of Hawaiian arthropods using ecological niche modelling.
553 Biological Journal of the Linnean Society *127*, 479-492.
554 3. Kozak, K.H., and Wiens, J.J. (2006). Does niche conservatism promote
555 speciation? A case study in North American salamanders. Evolution *60*, 2604-
556 2621.
557 4. Wiens, J.J. (2004). Speciation and ecology revisited: phylogenetic niche
558 conservatism and the origin of species. Evolution *58*, 193-197.
559 5. Rosenblum, E.B., Parent, C.E., and Brandt, E.E. (2014). The Molecular Basis of
560 Phenotypic Convergence. Annual Review of Ecology, Evolution, and Systematics,
561 Vol 45 *45*, 203-226.
562 6. Elmer, K.R., and Meyer, A. (2011). Adaptation in the age of ecological genomics:
563 insights from parallelism and convergence. Trends in Ecology & Evolution *26*,
564 298-306.
565 7. Jones, F.C., Grabherr, M.G., Chan, Y.F., Russell, P., Mauceli, E., Johnson, J.,
566 Swofford, R., Pirun, M., Zody, M.C., White, S., et al. (2012). The genomic basis of
567 adaptive evolution in threespine sticklebacks. Nature *484*, 55-61.
568 8. Faria, R., Renaut, S., Galindo, J., Pinho, C., Melo-Ferreira, J., Melo, M., Jones, F.,
569 Salzburger, W., Schluter, D., and Butlin, R. (2014). Advances in Ecological
570 Speciation: an integrative approach. Molecular Ecology *23*, 513-521.
571 9. Schluter, D., and McPhail, J.D. (1992). Ecological character displacement and
572 speciation in sticklebacks. American Naturalist *140*, 85-108.
573 10. Schluter, D. (1996). Ecological speciation in postglacial fishes. Philosophical
574 Transactions of the Royal Society of London Series B-Biological Sciences *351*,
575 807-814.
576 11. McGee, M.D., Schluter, D., and Wainwright, P.C. (2013). Functional basis of
577 ecological divergence in sympatric stickleback. Bmc Evolutionary Biology *13*.
578 12. Hendry, A.P. (2009). Ecological speciation! Or the lack thereof? Canadian Journal
579 of Fisheries and Aquatic Sciences *66*, 1383-1398.
580 13. Magalhaes, I.S., Whiting, J.R., D'Agostino, D., Hohenlohe, P.A., Mahmud, M.,
581 Bell, M.A., Skulason, S., and MacColl, A.D.C. (2021). Intercontinental genomic
582 parallelism in multiple three-spined stickleback adaptive radiations. Nature
583 Ecology & Evolution *5*, 251-261.
584 14. Arnegard, M.E., McGee, M.D., Matthews, B., Marchinko, K.B., Conte, G.L., Kabir,
585 S., Bedford, N., Bergek, S., Chan, Y.F., Jones, F.C., et al. (2014). Genetics of
586 ecological divergence during speciation. Nature *511*, 307-311.
587 15. McPhail, J.D. (1994). Speciation and the evolution of reproductive isolation in the
588 sticklebacks (*Gasterosteus*) of south-western British Columbia. In The
589 evolutionary biology of the threespine stickleback, M.A. Bell and S.A. Foster, eds.
590 (Oxford University Press).
591 16. McPhail, J.D. (1992). Ecology and evolution of sympatric sticklebacks
592 (*Gasterosteus*) - evidence for a species-pair in Paxton Lake, Texada island, British
593 Columbia. Canadian Journal of Zoology-Revue Canadienne De Zoologie *70*, 361-
594 369.
595 17. Gow, J.L., Rogers, S.M., Jackson, M., and Schluter, D. (2008). Ecological
596 predictions lead to the discovery of a benthic-limnetic sympatric species pair of
597 threespine stickleback in Little Quarry Lake, British Columbia. Canadian Journal of
598 Zoology-Revue Canadienne De Zoologie *86*, 564-571.
599 18. Schluter, D. (1995). Adaptive radiation in sticklebacks: trade-offs in feeding
600 performance and growth. Ecology *76*, 82-90.

bioRxiv preprint doi: https://doi.org/10.1101/2022.10.02.510516; this version posted October 4, 2022. The copyright holder for this preprint (which was not certified by peer review) is the author/funder, who has granted bioRxiv a license to display the preprint in perpetuity. It is made available under aCC-BY-NC-ND 4.0 International license.

19. Gow, J.L., Peichel, C.L., and Taylor, E.B. (2007). Ecological selection against hybrids in natural populations of sympatric threespine sticklebacks. Journal of Evolutionary Biology *20*, 2173-2180.
20. Hatfield, T., and Schluter, D. (1999). Ecological speciation in sticklebacks: environment-dependent hybrid fitness. Evolution *53*, 866-873.
21. Jones, F.C., Chan, Y.F., Schmutz, J., Grimwood, J., Brady, S.D., Southwick, A.M., Absher, D.M., Myers, R.M., Reimchen, T.E., Deagle, B.E., et al. (2012). A genome-wide SNP genotyping array reveals patterns of global and repeated species-pair divergence in sticklebacks. Current Biology *22*, 83-90.
22. Taylor, E.B., and McPhail, J.D. (2000). Historical contingency and ecological determinism interact to prime speciation in sticklebacks, *Gasterosteus*. Proceedings of the Royal Society B-Biological Sciences *267*, 2375-2384.
23. Vines, T.H., and Schluter, D. (2006). Strong assortative mating between allopatric sticklebacks as a by-product of adaptation to different environments. Proceedings of the Royal Society B-Biological Sciences *273*, 911-916.
24. Rundle, H.D., and Schluter, D. (1998). Reinforcement of stickleback mate preferences: sympatry breeds contempt. Evolution *52*, 200-208.
25. Taylor, E.B., and McPhail, J.D. (1999). Evolutionary history of an adaptive radiation in species pairs of threespine sticklebacks (*Gasterosteus*): insights from mitochondrial DNA. Biological Journal of the Linnean Society *66*, 271-291.
26. McPhail, J.D. (1993). Ecology and evolution of sympatric sticklebacks (*Gasterosteus*) - origin of the species pairs. Canadian Journal of Zoology-Revue Canadienne De Zoologie *71*, 515-523.
27. Taylor, E.B., Boughman, J.W., Groenenboom, M., Sniatynski, M., Schluter, D., and Gow, J.L. (2006). Speciation in reverse: morphological and genetic evidence of the collapse of a three-spined stickleback (*Gasterosteus aculeatus*) species pair. Molecular Ecology *15*, 343-355.
28. Gow, J.L., Peichel, C.L., and Taylor, E.B. (2006). Contrasting hybridization rates between sympatric three-spined sticklebacks highlight the fragility of reproductive barriers between evolutionarily young species. Molecular Ecology *15*, 739-752.
29. Bierne, N., Gagnaire, P.A., and David, P. (2013). The geography of introgression in a patchy environment and the thorn in the side of ecological speciation. Current Zoology *59*, 72-86.
30. McKinnon, J.S., and Rundle, H.D. (2002). Speciation in nature: the threespine stickleback model systems. Trends in Ecology & Evolution *17*, 480-488.
31. Harer, A., Bolnick, D.I., and Rennison, D.J. (2021). The genomic signature of ecological divergence along the benthic-limnetic axis in allopatric and sympatric threespine stickleback. Molecular Ecology *30*, 451-463.
32. Ingram, T., and Mahler, D.L. (2013). SURFACE: detecting convergent evolution from comparative data by fitting Ornstein-Uhlenbeck models with stepwise Akaike Information Criterion. Methods in Ecology and Evolution *4*, 416-425.
33. Malinsky, M., Trucchi, E., Lawson, D.J., and Falush, D. (2018). RADpainter and fineRADstructure Population Inference from RADseq Data. Molecular Biology and Evolution *35*, 1284-1290.
34. Kemppainen, P., Knight, C.G., Sarma, D.K., Hlaing, T., Prakash, A., Maung, Y.N.M., Somboon, P., Mahanta, J., and Walton, C. (2015). Linkage disequilibrium network analysis (LDna) gives a global view of chromosomal inversions, local adaptation and geographic structure. Molecular Ecology Resources *15*, 1031-1045.
35. Willacker, J.J., Von Hippel, F.A., Wilton, P.R., and Walton, K.M. (2010). Classification of threespine stickleback along the benthic-limnetic axis. Biological Journal of the Linnean Society *101*, 595-608.
36. Schluter, D. (1993). Adaptive radiation in sticklebacks - size, shape, and habitat use efficiency. Ecology *74*, 699-709.
37. Som, A. (2015). Causes, consequences and solutions of phylogenetic incongruence. Brief. Bioinform. *16*, 536-548.

bioRxiv preprint doi: https://doi.org/10.1101/2022.10.02.510516; this version posted October 4, 2022. The copyright holder for this preprint (which was not certified by peer review) is the author/funder, who has granted bioRxiv a license to display the preprint in perpetuity. It is made available under aCC-BY-NC-ND 4.0 International license.

38. Leache, A.D., Harris, R.B., Rannala, B., and Yang, Z.H. (2014). The Influence of Gene Flow on Species Tree Estimation: A Simulation Study. Systematic Biology *63*, 17-30.
39. Muenkemueller, T., Lavergne, S., Bzeznik, B., Dray, S., Jombart, T., Schiffers, K., and Thuiller, W. (2012). How to measure and test phylogenetic signal. Methods in Ecology and Evolution *3*, 743-756.
40. Wiens, J.J., Ackerly, D.D., Allen, A.P., Anacker, B.L., Buckley, L.B., Cornell, H.V., Damschen, E.I., Davies, T.J., Grytnes, J.-A., Harrison, S.P., et al. (2010). Niche conservatism as an emerging principle in ecology and conservation biology. Ecology Letters *13*, 1310-1324.
41. Buckley, L.B., Davies, T.J., Ackerly, D.D., Kraft, N.J.B., Harrison, S.P., Anacker, B.L., Cornell, H.V., Damschen, E.I., Grytnes, J.-A., Hawkins, B.A., et al. (2010). Phylogeny, niche conservatism and the latitudinal diversity gradient in mammals. Proceedings of the Royal Society B-Biological Sciences *277*, 2131-2138.
42. Fang, B.H., Kemppainen, P., Momigliano, P., Feng, X.Y., and Merila, J. (2020). On the causes of geographically heterogeneous parallel evolution in sticklebacks. Nature Ecology & Evolution *4*, 1105-+.
43. Degnan, J.H., and Rosenberg, N.A. (2009). Gene tree discordance, phylogenetic inference and the multispecies coalescent. Trends in Ecology & Evolution *24*, 332-340.
44. Conte, G.L., Arnegard, M.E., Best, J., Chan, Y.F., Jones, F.C., Kingsley, D.M., Schluter, D., and Peichel, C.L. (2015). Extent of QTL Reuse During Repeated Phenotypic Divergence of Sympatric Threespine Stickleback. Genetics *201*, 1189-U1730.
45. Erickson, P.A., Glazer, A.M., Killingbeck, E.E., Agoglia, R.M., Baek, J., Carsanaro, S.M., Lee, A.M., Cleves, P.A., Schluter, D., and Miller, C.T. (2016). Partially repeatable genetic basis of benthic adaptation in threespine sticklebacks. Evolution *70*, 887-902.
46. Ingram, T., Svanbaeck, R., Kraft, N.J.B., Kratina, P., Southcott, L., and Schluter, D. (2012). Intraguild predation drives evolutionary niche shift in threespine stickleback. Evolution *66*, 1819-1832.
47. Edwards, S.V. (2009). Natural selection and phylogenetic analysis. Proceedings of the National Academy of Sciences of the United States of America *106*, 8799-8800.
48. Miller, S.E., Roesti, M., and Schluter, D. (2019). A Single Interacting Species Leads to Widespread Parallel Evolution of the Stickleback Genome. Current Biology *29*, 530-537.
49. Miller, S.E., Metcalf, D., and Schluter, D. (2015). Intraguild predation leads to genetically based character shifts in the threespine stickleback. Evolution *69*, 3194-3203.
50. Castoe, T.A., de Koning, A.P.J., Kim, H.-M., Gu, W., Noonan, B.P., Naylor, G., Jiang, Z.J., Parkinson, C.L., and Pollock, D.D. (2009). Evidence for an ancient adaptive episode of convergent molecular evolution. Proceedings of the National Academy of Sciences of the United States of America *106*, 8986-8991.
51. Edwards, S.V., Xi, Z.X., Janke, A., Faircloth, B.C., McCormack, J.E., Glenn, T.C., Zhong, B.J., Wu, S.Y., Lemmon, E.M., Lemmon, A.R., et al. (2016). Implementing and testing the multispecies coalescent model: A valuable paradigm for phylogenomics. Molecular Phylogenetics and Evolution *94*, 447-462.
52. Adams, R.H., Schield, D.R., Card, D.C., and Castoe, T.A. (2018). Assessing the Impacts of Positive Selection on Coalescent-Based Species Tree Estimation and Species Delimitation. Systematic Biology *67*, 1076-1090.
53. Clague, J.J., Roberts, N.J., Miller, B., Menounos, B., and Goehring, B. (2021). A huge flood in the Fraser River valley, British Columbia, near the Pleistocene Termination. Geomorphology *374*.
54. Lescak, E.A., Bassham, S.L., Catchen, J., Gelmond, O., Sherbick, M.L., von Hippel, F.A., and Cresko, W.A. (2015). Evolution of stickleback in 50 years on

bioRxiv preprint doi: https://doi.org/10.1101/2022.10.02.510516; this version posted October 4, 2022. The copyright holder for this preprint (which was not certified by peer review) is the author/funder, who has granted bioRxiv a license to display the preprint in perpetuity. It is made available under aCC-BY-NC-ND 4.0 International license.

earthquake-uplifted islands. Proceedings of the National Academy of Sciences of the United States of America *112*, E7204-E7212.

55. Kitano, J., Bolnick, D.I., Beauchamp, D.A., Mazur, M.M., Mori, S., Nakano, T., and Peichel, C.L. (2008). Reverse evolution of armour plates in threespine stickleback. Current Biology *18*, 769-774.

56. Aguirre, W.E., and Bell, M.A. (2012). Twenty years of body shape evolution in a threespine stickleback population adapting to a lake environment. Biological Journal of the Linnean Society *105*, 817-831.

57. Terekhanova, N.V., Logacheva, M.D., Penin, A.A., Neretina, T.V., Barmintseva, A.E., Bazykin, G.A., Kondrashov, A.S., and Mugue, N.S. (2014). Fast Evolution from Precast Bricks: Genomics of Young Freshwater Populations of Threespine Stickleback Gasterosteus aculeatus. Plos Genetics *10*.

58. Roberts Kingman, G.A., Vyas, D.N., Jones, F.C., Brady, S.D., Chen, H.I., Reid, K., Milhaven, M., Bertino, T.S., Aguirre, W.E., Heins, D.C., et al. (2021). Predicting future from past: The genomic basis of recurrent and rapid stickleback evolution. Science advances *7*.

59. Peichel, C.L., and Marques, D.A. (2017). The genetic and molecular architecture of phenotypic diversity in sticklebacks. Philosophical transactions of the Royal Society of London. Series B, Biological sciences *372*, 20150486.

60. HabitatWizard (accessed 27th Jan 2020). The Official Website of the Government of British Columbia. (Government of British Columbia).

61. Vamosi, S.M. (2003). The presence of other fish species affects speciation in threespine sticklebacks. Evolutionary Ecology Research *5*, 717-730.

62. Vamosi, S.M., and Schluter, D. (2002). Impacts of trout predation on fitness of sympatric sticklebacks and their hybrids. Proceedings of the Royal Society B-Biological Sciences *269*, 923-930.

63. James, G.D., and Kelso, J.R.M. (1995). Movements and habitat preference of adult rainbow trout (Oncorhynchus mykiss) in a New Zealand montane lake. New Zealand Journal of Marine and Freshwater Research *29*, 493-503.

64. Hutchinson, J.J., Pascoe, J., Smulders, M., Francis, D., and Fletcher, L. (2020). Kennedy Watershed Restoration Project 2014/2015 Completion Report. (Central Westcoast Forest Society).

65. Atkinson, J. (2016). Sproat Lake Adfluvial Piscivorous Cutthroat Trout Stock Assessment: Via Experimental Method Horizontal Limnetic Gillnets. (British Columbia: British Columbia Conservation Foundation).

66. Dennenmoser, S., Nolte, A.W., Vamosi, S.M., and Rogers, S.M. (2015). Phylogeography of the prickly sculpin (Cottus asper) in north-western North America reveals parallel phenotypic evolution across multiple coastal-inland colonizations. Journal of Biogeography *42*, 1626-1638.

67. Haenel, Q., Roesti, M., Moser, D., Maccoll, A.D.C., and Berner, D. (2019). Predictable genome-wide sorting of standing genetic variation during parallel adaptation to basic versus acidic environments in stickleback fish. Evolution Letters *0*, 1-15.

68. Giles, N. (1983). The possible role of environmental calcium levels during the evolution of phenotypic diversity in Outer Hebridean populations of the three-spined stickleback, *Gasterosteus aculeatus*. Journal of Zoology *199*, 535-544.

69. Rohlf, F.J. (2010). TpsDig, version 2.16. Department of Ecology and Evolution, State University of New York at Stony Brook, Available at http://life.bio.sunysb.edu/morph/.

70. Klingenberg, C.P. (2011). MorphoJ: an integrated software package for geometric morphometrics. Molecular Ecology Resources *11*, 353-357.

71. Reist, J.D. (1986). An empirical-evaluation of coefficients used in residual and allometric adjustment of size covariation. Canadian Journal of Zoology-Revue Canadienne De Zoologie *64*, 1363-1368.

72. R.Core.Team (2018). R: a language and environment for statistical computing. Version 3.5.2 Edition. (Vienna, Austria: R Foundation for Statistical Computing).

bioRxiv preprint doi: https://doi.org/10.1101/2022.10.02.510516; this version posted October 4, 2022. The copyright holder for this preprint (which was not certified by peer review) is the author/funder, who has granted bioRxiv a license to display the preprint in perpetuity. It is made available under aCC-BY-NC-ND 4.0 International license.

73. Peichel, C.L., Nereng, K.S., Ohgi, K.A., Cole, B.L.E., Colosimo, P.F., Buerkle, C.A., Schluter, D., and Kingsley, D.M. (2001). The genetic architecture of divergence between threespine stickleback species. Nature *414*, 901-905.
74. Schneider, C.A., Rasband, W.S., and Eliceiri, K.W. (2012). NIH Image to ImageJ: 25 years of image analysis. Nature Methods *9*, 671-675.
75. Magalhaes, I.S., Agostino, D.D., Hohenlohe, P.A., and Maccoll, A.D.C. (2016). The ecology of an adaptive radiation of three-spined stickleback from North Uist, Scotland. Molecular Ecology *25*, 4319-4336.
76. Catchen, J., Hohenlohe, P.A., Bassham, S., Amores, A., and Cresko, W.A. (2013). Stacks: an analysis tool set for population genomics. Molecular Ecology *22*, 3124-3140.
77. Danecek, P., Auton, A., Abecasis, G., Albers, C.A., Banks, E., DePristo, M.A., Handsaker, R.E., Lunter, G., Marth, G.T., Sherry, S.T., et al. (2011). The variant call format and VCFtools. Bioinformatics *27*, 2156-2158.
78. Chang, C.C., Chow, C.C., Tellier, L.C.A.M., Vattikuti, S., Purcell, S.M., and Lee, J.J. (2015). Second-generation PLINK: rising to the challenge of larger and richer datasets. Gigascience *4*.
79. Jombart, T. (2008). adegenet: a R package for the multivariate analysis of genetic markers. Bioinformatics *24*, 1403-1405.
80. Lawson, D.J., Hellenthal, G., Myers, S., and Falush, D. (2012). Inference of Population Structure using Dense Haplotype Data. Plos Genetics *8*.
81. Lischer, H.E.L., and Excoffier, L. (2012). PGDSpider: an automated data conversion tool for connecting population genetics and genomics programs. Bioinformatics *28*, 298-299.
82. Bell, M.A., and Foster, S.A. (1994). Introduction to the evolutionary biology of the threespine stickleback. In The evolutionary biology of the threespine stickleback, M.A. Bell and S.A. Foster, eds. (Oxford University Press), pp. 1-27.
83. Pinheiro, J., Bates, D., DebRoy, S., Sarkar, D., and Team, t.R.D.C. (2018). nlme: Linear and Nonlinear Mixed Effects Models. R package version 3.1-137.
84. Lenth, R. (2019). emmeans: Estimated Marginal Means, aka Least-Squares Means. R package version 1.3.3.
85. Benjamini, Y., and Hochberg, Y. (1995). Controlling the false discovery rate: a practical and powerful approach to multiple testing. Journal of the Royal Statistical Society Series B-Statistical Methodology *57*, 289-300.
86. Stamatakis, A. (2014). RAxML version 8: a tool for phylogenetic analysis and post-analysis of large phylogenies. Bioinformatics *30*, 1312-1313.
87. Martin, S.H., and Van Belleghem, S.M. (2017). Exploring Evolutionary Relationships Across the Genome Using Topology Weighting. Genetics *206*, 429-438.
88. Guindon, S., Dufayard, J.-F., Lefort, V., Anisimova, M., Hordijk, W., and Gascuel, O. (2010). New Algorithms and Methods to Estimate Maximum-Likelihood Phylogenies: Assessing the Performance of PhyML 3.0. Systematic Biology *59*, 307-321.
89. Paradis, E., and Schliep, K. (2019). ape 5.0: an environment for modern phylogenetics and evolutionary analyses in R. Bioinformatics *35*, 526-528.
90. Revell, L.J. (2012). phytools: an R package for phylogenetic comparative biology (and other things). Methods in Ecology and Evolution *3*, 217-223.
91. Schliep, K.P. (2011). phangorn: phylogenetic analysis in R. Bioinformatics *27*, 592-593.
92. Keck, F., Rimet, F., Bouchez, A., and Franc, A. (2016). phylosignal: an R package to measure, test, and explore the phylogenetic signal. Ecology and Evolution *6*, 2774-2780.
93. Pagel, M. (1999). Inferring the historical patterns of biological evolution. Nature *401*, 877-884.
94. Freckleton, R.P., Harvey, P.H., and Pagel, M. (2002). Phylogenetic analysis and comparative data: A test and review of evidence. American Naturalist *160*, 712-726.

bioRxiv preprint doi: https://doi.org/10.1101/2022.10.02.510516; this version posted October 4, 2022. The copyright holder for this preprint (which was not certified by peer review) is the author/funder, who has granted bioRxiv a license to display the preprint in perpetuity. It is made available under aCC-BY-NC-ND 4.0 International license.

826 95. Molina-Venegas, R., and Rodriguez, M.A. (2017). Revisiting phylogenetic signal;
827 strong or negligible impacts of polytomies and branch length information? Bmc
828 Evolutionary Biology *17*.
829 96. Pinheiro, J., Bates, D., DebRoy, S., Sarkar, D., and Team, t.R.D.C. (2018). nlme:
830 Linear and Nonlinear Mixed Effects Models. R package version 3.1-137.
831 97. Harmon, L.J., Weir, J.T., Brock, C.D., Glor, R.E., and Challenger, W. (2008).
832 GEIGER: investigating evolutionary radiations. Bioinformatics *24*, 129-131.
833 98. Mazel, F., Davies, T.J., Georges, D., Lavergne, S., Thuiller, W., and Peres-Neto,
834 P.R. (2016). Improving phylogenetic regression under complex evolutionary
835 models. Ecology *97*, 286-293.

836

Supplementary Tables

Table S1

Description of sample sites. Sample sizes are shown for phenotypic (n pheno) and RAD (n RAD) analyses. Sal refers to salinity classifications, Fr: freshwater (absolute conductivity <500 μS/cm), Br: brackish (absolute conductivity 20,000-35,000 μS/cm). Sampling locations are given by latitude followed by longitude.

Lake ID	Lake name	n pheno	n RAD	Genomic cluster	Mean depth (m)	Area (km^2)	Sculpin	Sal	Location
AMBR	Ambrose lake	29	17	1	13.3	0.2980	Yes	Fr	49°44'3"N; 124°1'16"W
BEAV	Beaver lake	30	19	1	3.5	0.1932	Yes	Fr	48°48'42"N; 124° 4'51"W
BRAN	Brannen lake	30	19	2	11.6	1.0866	Yes	Fr	49°12'55"N; 124°3'18"W
BULL	Bullocks lake	30	17	2	4.0	0.0940	No	Fr	48°52'25N; 123°30'33"W
CRAN	Cranby lake	30	20	2	3.2	0.4460	No	Fr	49°41'36"N; 124°30'42"W
DOUG	Dougan lake	30	16	2	8.5	0.1000	No	Fr	48°42'53"N; 123°36'48"W
GARD	Garden bay	10	9	1	10.0	0.6236	Yes	Fr	49°39'1"N; 124°1'23"W
HOGG	Hoggan lake	30	20	2	3.0	0.1970	No	Fr	49°9'7"N; 123°49'43"W
HOTE	Hotel	35	17	1	5.9	0.2522	No	Fr	49°38'26"N; 124°3'3"W
KENN	Kennedy lake	30	19	1	38.0	65.0000	Yes	Fr	49°3'59"N; 125°28'2"W
KIRK	Kirk lake	30	18	2	8.3	0.0830	No	Fr	49°44'22"N; 124°34'57"W
KLEN	Klein lake	30	17	2	12.0	0.1350	No	Fr	49°43'53"N; 123°58'23"W
LICA	Little Campbell river	34	10	1	3.0	74.400	Yes	Br	49°0'51"N; 122°45'32"W
LILY	Lily lake	30	19	1	2.2	0.1214	Yes	Fr	49°36'44"N; 124° 1'17"W
NORT	North lake	14	14	1	10.1	0.1279	Yes	Fr	49°44'60"N; 123°58'27"W
OYST	Oyster lagoon	30	10	1	1.3	0.0200	Yes	Br	49°36'49"N; 124°1'47"W
PAXT	Paxton lake	63	9	1 / 2	6.2	0.1700	No	Fr	49°42'22"N; 124°31'24"W
PRIE	Priest lake	57	9	1 / 2	5.4	0.4434	No	Fr	49°44'50"N; 124°33'52"W
SPRO	Sproat lake	30	19	1	65.5	37.7500	Yes	Fr	49°16'0"N; 125°2'13"W
STOW	Stowell lake	30	17	2	4.6	0.0564	No	Fr	48°46'54"N; 123°26'37"W
TROU	Trout lake	30	18	2	5.8	0.0756	No	Fr	49°30'26"N; 123°52'37"W

bioRxiv preprint doi: https://doi.org/10.1101/2022.10.02.510516; this version posted October 4, 2022. The copyright holder for this preprint (which was not certified by peer review) is the author/funder, who has granted bioRxiv a license to display the preprint in perpetuity. It is made available under aCC-BY-NC-ND 4.0 International license.

Table S2

SNPs in linkage cluster 10 that lie within genes. Genome location of SNPs falling within coding regions and the associated gene and gene ID for each SNP.

Chromosome	SNP	Gene name	Ensembl gene ID
groupI	138067		ENSGACG00000004458
groupI	1913469		ENSGACG00000005744
groupI	14210802		ENSGACG00000011908
groupI	22123269		ENSGACG00000014464
groupII	20248077	NELL1	ENSGACG00000017098
groupIV	4186906	pde6a	ENSGACG00000016811
groupV	291741	kat6b	ENSGACG00000002173
groupV	1957242	glud1b	ENSGACG00000002813
groupV	2216160	cyth1b	ENSGACG00000002991
groupVI	2259976	cpeb3	ENSGACG00000002944
groupVI	6422836	fbxolla	ENSGACG00000005432
groupVI	13171573	sdccag8	ENSGACG00000010549
groupVII	20193529	dclk1a	ENSGACG00000020560
groupX	8795111	fam126a	ENSGACG00000006077
groupXIII	9178337	ube3b	ENSGACG00000009166
groupXIII	15603103	arvcfb	ENSGACG00000013003
groupXIII	17477236	krt1-c5	ENSGACG00000013907
groupXIV	4013936	dnajc21	ENSGACG00000016480
groupXV	9968890	ppp2r3a	ENSGACG00000010930
groupXV	14295031	odc1	ENSGACG00000012974
groupXVI	119418		ENSGACG00000001436
groupXVI	210791	pde9a	ENSGACG00000001450
groupXVII	840001	ccdc51	ENSGACG00000003571
groupXVII	6327443	trim62.1	ENSGACG00000007462
groupXXI	2692493	nrros	ENSGACG00000002094
scaffold_114	90942	itpr3	ENSGACG00000000253
scaffold_114	90942		ENSGACG00000000233
scaffold_27	3558934	wdr82	ENSGACG00000001254

bioRxiv preprint doi: https://doi.org/10.1101/2022.10.02.510516; this version posted October 4, 2022. The copyright holder for this preprint (which was not certified by peer review) is the author/funder, who has granted bioRxiv a license to display the preprint in perpetuity. It is made available under aCC-BY-NC-ND 4.0 International license.

847 **Table S3**

848 **Linear mixed model results for phenotypic differences between groups.** Table shows the
849 results of linear mixed models testing for differences between three groups (marine, genomic
850 cluster 1 and genomic cluster 2) in five phenotypic traits, with population as a random effect.

Trait	*F*	*df*	*p*-value
Weight	4.4219	2	0.0257
N gill rakers	5.4898	2	0.0126
Raker length	12.4074	2	0.0003
Armour PC1	8.1948	2	0.0025
Shape PC1	23.0643	2	<0.0001

851 *F* describes the likelihood ratio test statistic, *df* describes degrees of freedom. *P*-values < 0.05
852 are highlighted in bold.

bioRxiv preprint doi: https://doi.org/10.1101/2022.10.02.510516; this version posted October 4, 2022. The copyright holder for this preprint (which was not certified by peer review) is the author/funder, who has granted bioRxiv a license to display the preprint in perpetuity. It is made available under aCC-BY-NC-ND 4.0 International license.

Table S4

Post-hoc Estimated marginal means test results for pairwise phenotypic differences between groups. Table shows the results of post-hoc estimated marginal means tests to determine pairwise differences between groups (marine, genomic cluster 1 and genomic cluster 2) when phenotypes differed significantly between groups in linear mixed models.

Trait	Groups compared	Estimate	SE	*df*	Adjusted *p*-value
Weight	limnetic-like – benthic-like	0.2453	0.2400	20	0.3188
	marine – benthic-like	-1.0119	0.4193	20	**0.0383**
	marine – limnetic-like	-1.2572	0.4232	20	**0.0227**
N gill rakers	limnetic-like – benthic-like	-2.0254	0.6387	20	**0.0144**
	marine – benthic-like	-1.9978	1.1211	20	0.1349
	marine – limnetic-like	0.0276	1.1304	20	0.9808
Raker length	limnetic-like – benthic-like	-0.1799	0.0639	20	**0.0107**
	marine – benthic-like	-0.5286	0.1121	20	**0.0004**
	marine – limnetic-like	-0.3487	0.1130	20	**0.0088**
Armour PC1	limnetic-like – benthic-like	-2.2551	0.6914	20	**0.0069**
	marine – benthic-like	-3.8791	1.2155	20	**0.0069**
	marine – limnetic-like	-1.6240	1.2250	20	0.1999
Shape PC1	limnetic-like – benthic-like	-2.4654	0.4697	20	**<0.0001**
	marine – benthic-like	-4.5652	0.8202	20	**<0.0001**
	marine – limnetic-like	-2.0998	0.8280	20	**0.0197**

Estimates describe the mean difference between groups, SE describes the standard error of the estimates and *df* describe degrees of freedom. *P*-values are adjusted for multiple testing using the FDR method. *P*-values < 0.05 are highlighted in bold.

bioRxiv preprint doi: https://doi.org/10.1101/2022.10.02.510516; this version posted October 4, 2022. The copyright holder for this preprint (which was not certified by peer review) is the author/funder, who has granted bioRxiv a license to display the preprint in perpetuity. It is made available under aCC-BY-NC-ND 4.0 International license.

Table S5

Effects of the environment on the distribution of benthic-limnetic phenotypic traits. Table shows the results of phylogenetic generalised least squares analyses (PGLS) on each phenotypic trait. *P*-values < 0.05 are highlighted in bold. *P*-values were adjusted for multiple testing using the FDR method.

Phenotypic trait	Environmental variable	*df*	Wald statistic	*p*-value	Adjusted *p*-value
Armour PC1	Lake area	1	1.5877	0.2077	0.5077
	Ca concentration	1	3.2274	0.0724	0.2172
	Mean lake depth	1	0.0883	0.7663	0.8969
	pH	1	1.6609	0.1975	0.3950
	Sculpin presence	1	17.6411	**0.0000**	**0.0002**
N rakers	Lake area	1	0.0461	0.8300	0.8300
	Ca concentration	1	0.3525	0.5527	0.6088
	Mean lake depth	1	0.0327	0.8564	0.8969
	pH	1	0.1860	0.6663	0.7882
	Sculpin presence	1	0.7284	0.3934	0.4721
Raker length	Lake area	1	6.8857	**0.0087**	0.0521
	Ca concentration	1	1.4304	0.2317	0.4634
	Mean lake depth	1	0.0168	0.8969	0.8969
	pH	1	0.5091	0.4755	0.7133
	Sculpin presence	1	2.6932	0.1008	0.1512
Shape PC1	Lake area	1	0.0641	0.8001	0.8300
	Ca concentration	1	0.2620	0.6088	0.6088
	Mean lake depth	1	0.1346	0.7137	0.8969
	pH	1	1.7163	0.1902	0.3950
	Sculpin presence	1	3.8490	**0.0498**	0.0996
Weight	Lake area	1	0.1549	0.6939	0.8300
	Ca concentration	1	0.5770	0.4475	0.6088
	Mean lake depth	1	16.8205	**0.0002**	**0.0013**
	pH	1	7.9713	**0.0048**	**0.0285**
	Sculpin presence	1	0.0013	0.9714	0.9714

bioRxiv preprint doi: https://doi.org/10.1101/2022.10.02.510516; this version posted October 4, 2022. The copyright holder for this preprint (which was not certified by peer review) is the author/funder, who has granted bioRxiv a license to display the preprint in perpetuity. It is made available under aCC-BY-NC-ND 4.0 International license.

867 **Supplementary Figures**

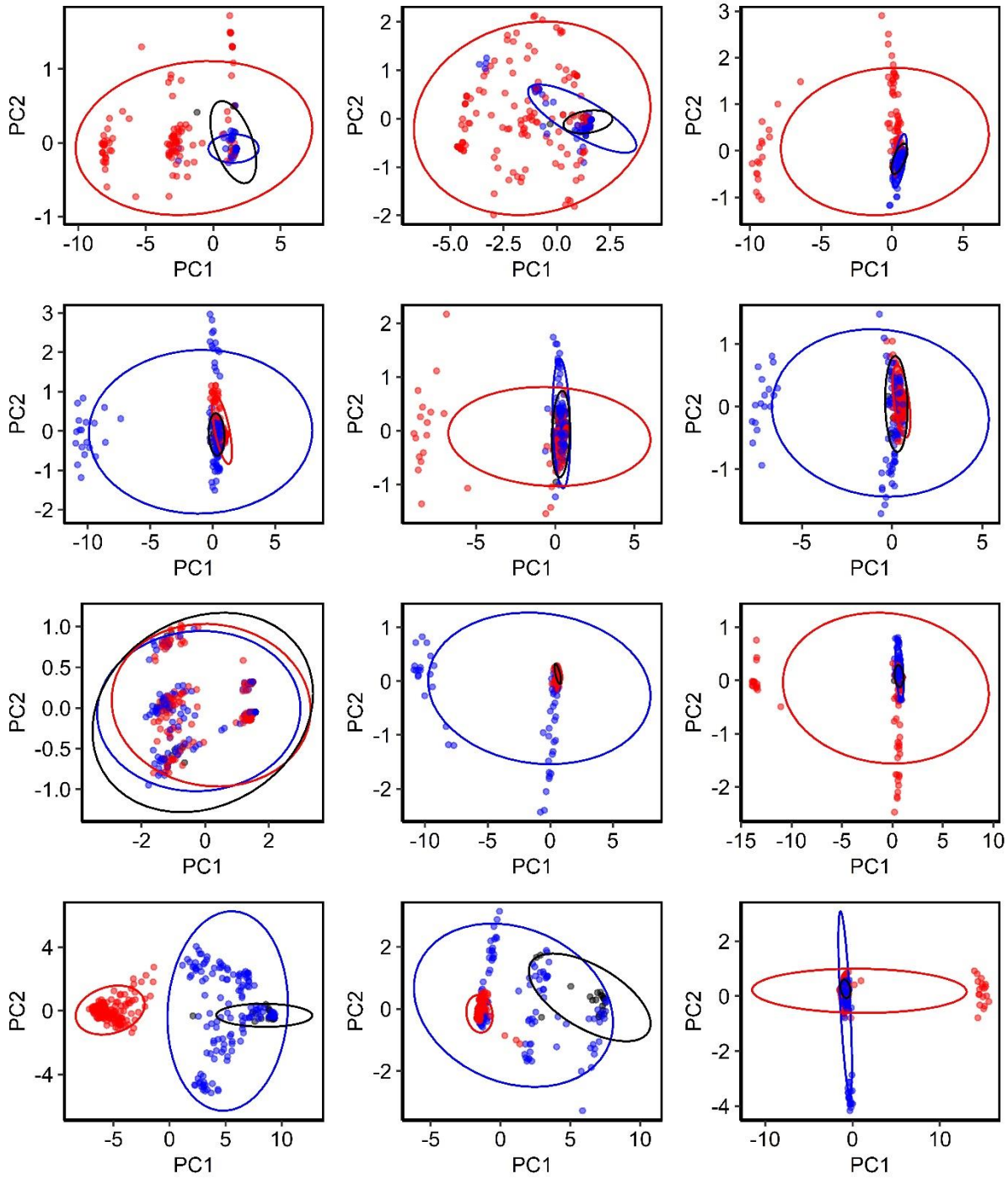

868

869 **Figure S1.** Principal component analyses (PCA) of each LD cluster in the LD network
870 identified by LDna. Black circles represent marine individuals, blue circles, freshwater
871 cluster 1 and red circles freshwater cluster 2. 95% confidence ellipses are shown for each
872 PCA in the corresponding colours.

bioRxiv preprint doi: https://doi.org/10.1101/2022.10.02.510516; this version posted October 4, 2022. The copyright holder for this preprint (which was not certified by peer review) is the author/funder, who has granted bioRxiv a license to display the preprint in perpetuity. It is made available under aCC-BY-NC-ND 4.0 International license.

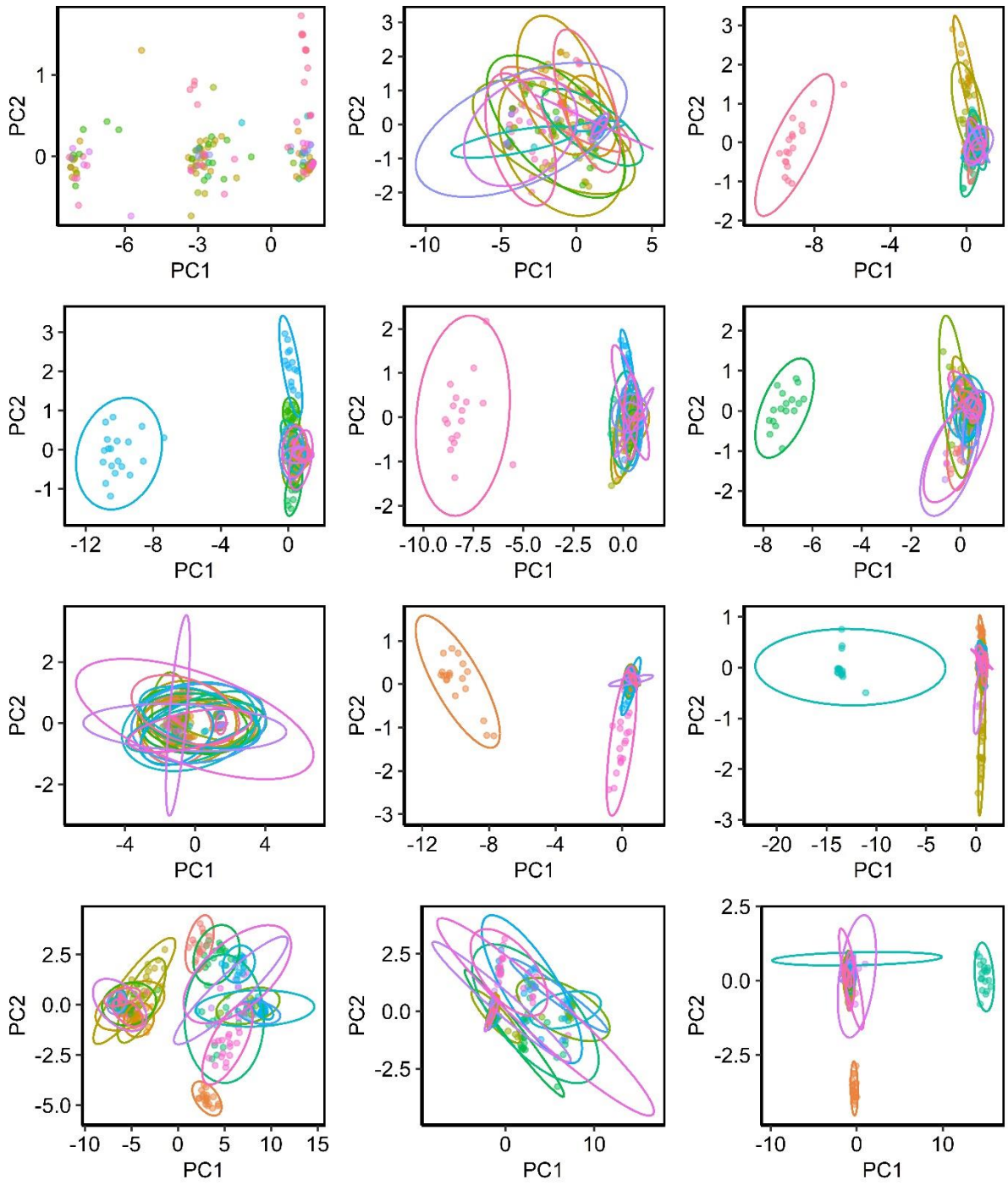

873

874 **Figure S2.** Principal component analyses (PCA) of each LD cluster in the LD network
875 identified by LDna. Coloured circles and ellipses represent each of the 23 sampled
876 populations.